Evaluation Method of TiO_2-SiO_2 Ultra-Low-Expansion Glasses with Periodic Striae Using the LFB Ultrasonic Material Characterization System

Jun-ichi Kushibiki, *Member, IEEE*, Mototaka Arakawa, *Member, IEEE*, Yuji Ohashi, *Member, IEEE*, and Kouji Suzuki

***Abstract*—Experimental procedures and standard specimens for characterizing and evaluating TiO_2-SiO_2 ultra-low expansion glasses with periodic striae using the line-focus-beam (LFB) ultrasonic material characterization system are discussed. Two types of specimens were prepared, with specimen surfaces parallel and perpendicular to the striae plane using two different grades of glass ingots. The inhomogeneities of each of the specimens were evaluated at 225 MHz. It was clarified that parallel specimens are useful for accurately measuring velocity variations of leaky surface acoustic waves (LSAWs) excited on a water-loaded specimen surface associated with the striae. Perpendicular specimens are useful for obtaining periodicities in the striae for LSAW propagation perpendicular to the striae plane on a surface and for precisely measuring averaged velocities for LSAW propagation parallel to the striae plane. The standard velocity of Rayleigh-type LSAWs traveling parallel to the striae plane for the perpendicular specimens was numerically calculated using the measured velocities of longitudinal and shear waves and density. Consequently, a reliable standard specimen with an LSAW velocity of 3308.18 ± 0.35 m/s at 23°C and its temperature coefficient of 0.39 (m/s)/°C was obtained for a TiO_2-SiO_2 glass with a TiO_2 concentration of 7.09 wt%. A basis for the striae analysis using this ultrasonic method was established.**

I. Introduction

Ultra-low expansion glasses have smaller coefficients of thermal expansion (CTE) than synthetic silica glass (400 to 550 ppb/K [1][1]) and have been used as materials for lenses and mirrors in large astronomical telescopes and satellites situated in special temperature environments. They are commercially available, and their leading products include ULE® (C-7971/7972), TiO_2-doped SiO_2 (TiO_2-SiO_2) glass [2], [3] manufactured by Corning Inc., Corning, NY, and Zerodur®, Li_2O-Al_2O_3-SiO_2 crystallized glass [4], [5] produced by Schott AG, Mainz, Germany. The former has achieved an ultra-low CTE by adjusting the concentration ratio of TiO_2 and SiO_2, and the latter by adjusting chemical composition ratios of 10 elements [5] and the conditions of the crystallization process (temperature and time). In the fabrication of glasses with the desired CTE characteristics, it is essential that the properties of the glass are accurately evaluated and that the obtained information is effectively fed back to improve the fabrication process. Precise measurement of the acoustic properties of glasses is extremely useful for analyses and characterization of glass materials because the acoustic properties of glasses vary extensively depending on the chemical compositions and fabrication processes of the glasses and are closely related to their other chemical and physical properties [6]–[13]. Corning Inc. uses the velocity of longitudinal waves in its evaluation and selection of ULE® because the longitudinal velocity for TiO_2-SiO_2 glass is proportional to CTE [14]–[16].

We proposed a technique for analyzing and evaluating glass materials using the line-focus-beam ultrasonic material characterization (LFB-UMC) system [17], [18]. This technique allows a nondestructive, noncontact, two-dimensional analysis of the characteristics of the specimen surface by precisely measuring the phase velocity of leaky surface acoustic waves (LSAWs) propagating on a water-loaded specimen surface. We demonstrated its usefulness and effectiveness through various applications to scientific and industrial research into glasses. These include the evaluation of the homogeneity of glass substrates for surface acoustic wave (SAW) devices [19], [20], the formation of analytical relationships between acoustic properties and dopant concentrations in acoustic fibers [21], the characterization of optical fiber preforms [22], evaluation of the fabrication processes of silica glasses [23]–[25], and the development of an evaluation method for glass materials [26]. We recently extended application of this technique to a new evaluation method of the CTE of ultra-low expansion glasses for extreme ultra-violet lithography [27], [28].

LSAW velocity values measured with the LFB-UMC system vary according to the systems and ultrasonic devices used for measurements and their operating ultrasonic frequencies [29]. Therefore, the absolute values of the LSAW velocity are obtained by correcting the measured values through a system calibration method that uses a standard specimen with acoustical physical constants (elastic constants and density for nonpiezoelectric

Manuscript received February 20, 2006; accepted May 1, 2006. This work was supported in part by a Research Grant-in-Aid for the 21st COE (Center of Excellence) Program funded by the Japanese Ministry of Education, Culture, Sports, Science and Technology.

The authors are with the Department of Electrical Engineering, Tohoku University, Sendai 980-8579, Japan (e-mail: kushi@ecei.tohoku.ac.jp).

[1]Technical data of C-7980 glass from Corning Inc.

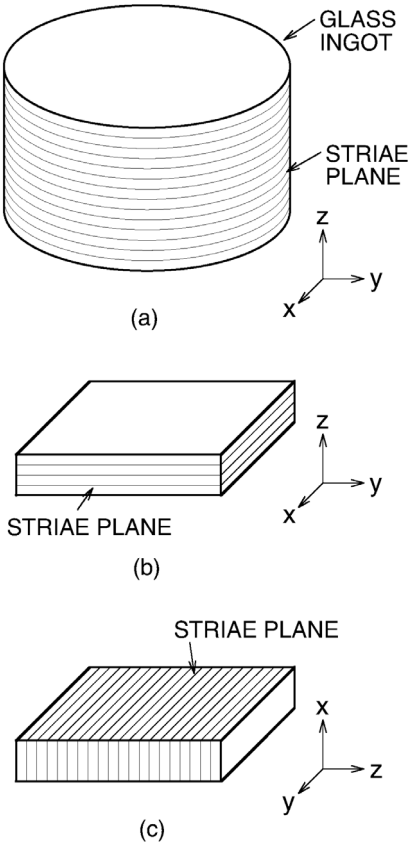

Fig. 1. Specimen preparation. (a) Glass ingot. (b) Specimen with the substrate surface prepared parallel to the striae plane (parallel specimen). (c) Specimen with the substrate surface prepared perpendicular to the striae plane (perpendicular specimen).

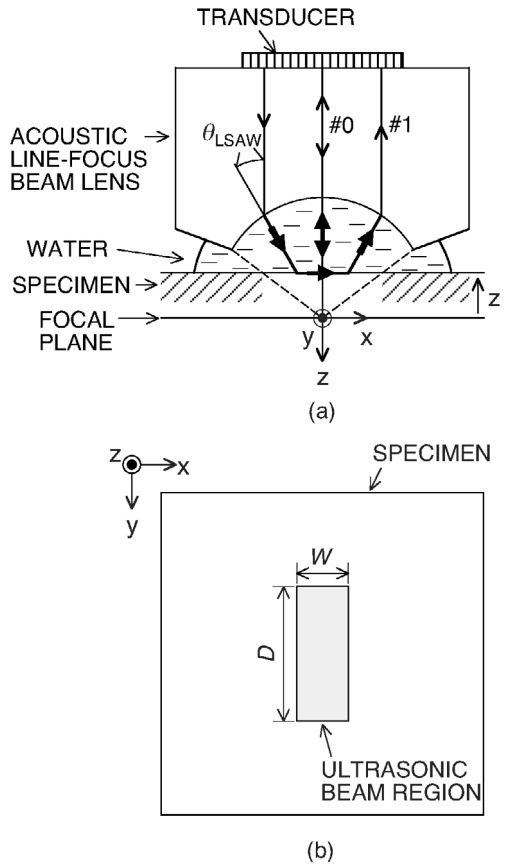

Fig. 2. (a) Cross-sectional geometry of the LFB ultrasonic device describing the principle of V(z) curve measurements. (b) Measurement region of the LFB at a specific defocus distance formed on the specimen.

materials) have been accurately measured [30]–[32]. The standard specimen in this method is ideally homogeneous because the calibration is made by comparing the actual measured LSAW velocity on the standard specimen with the calculated one obtained through numerical calculation using its measured bulk properties, viz., elastic constants, and density. However, it may be difficult to obtain the standard used to calibrate the measured velocities for inhomogeneous glass specimens, such as TiO_2-SiO_2 glass with periodic striae associated with its fabrication process [33] because of variations in the LSAW velocity measured at different positions.

To establish our method and system for striae evaluation of the TiO_2-SiO_2 glass, it is of fundamental importance to make analytical procedures of how to consider the periodic striae interacting with the LSAWs used for the V(z) curve measurements and how to prepare proper standard specimens. In this paper, we study these problems and examine the LSAW propagation characteristics in detail.

II. Specimens

Specimens were prepared from two commercially available ingots (1500 $mm^{\phi} \times 150$ mm^{t}) of TiO_2-SiO_2 ultra-low expansion glass (C-7972, Corning Inc.) of different grades (premium and mirror) in which the superscripts ϕ and t mean diameter and thickness of the circular plate. The specifications of these ingots provided in the catalog state that the absolute value of CTE is 0 ± 30 ppb/K and that the homogeneities are within 10 ppb/K for the premium-grade ingot and 15 ppb/K for the mirror-grade ingot. It has been reported that striae are formed in TiO_2-SiO_2 glass during the fabrication process and their periodicity is approximately 160 μm [33]. We prepared two types of specimen substrates cut from the ingots with the striae plane perpendicular to the z axis, as shown in Fig. 1(a), to investigate standard specimens suitable for precise system calibration; the substrate surfaces were parallel and perpendicular to the striae plane, as shown in Figs. 1(b) (parallel specimen) and 1(c) (perpendicular specimen). The substrates cut parallel and perpendicular to the striae plane of the premium-grade ingot (referred to as ingot A) were taken as specimen A-1 (46 mm $\times$ 60 mm $\times$ 4.8 mm^{t}) and specimen A-2 (61 mm $\times$ 47 mm $\times$ 4.8 mm^{t}), and those for the mirror-grade ingot (referred to as ingot B) were taken as parallel specimen B-1 (30 mm $\times$ 100 mm $\times$ 4.8 mm^{t}) and perpendicular specimen B-2 (55 mm $\times$ 50 mm $\times$ 4.8 mm^{t}). All specimens were optically polished on both sides with parallelisms within $10''$.

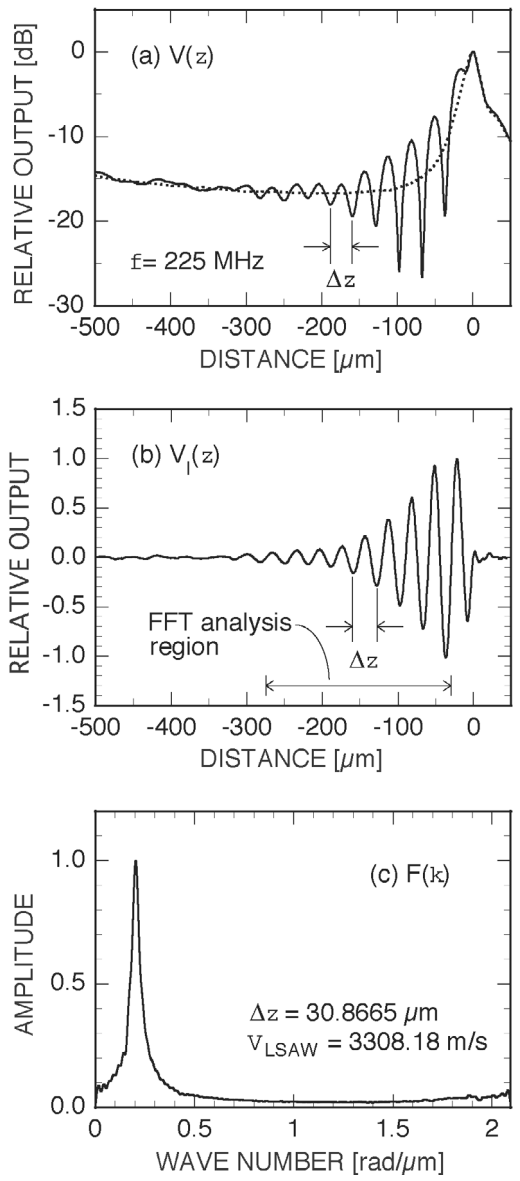

Fig. 3. V(z) curve analysis for the LSAW mode of C-7972 specimens at 225 MHz. (a) Typical V(z) curve and characteristic lens response $V_L(z)$ (dotted line). (b) Interference waveform of $V_I(z)$ curve. (c) Spectral distribution analyzed by FFT for the $V_I(z)$ curve shown in (b).

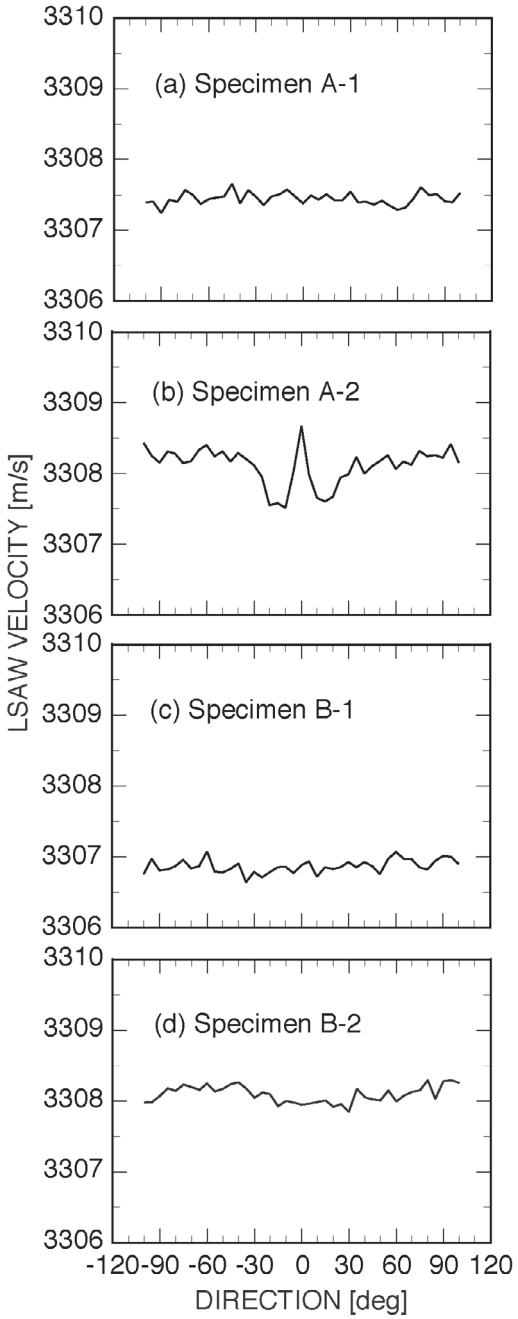

Fig. 4. Angular dependences of LSAW velocities for specimens A-1, A-2, B-1, and B-2 of C-7972 glass at 225 MHz.

III. LFB-UMC System and Measurement Region

Each specimen was measured at an ultrasonic frequency f of 225 MHz using the LFB-UMC system [18]. The measurement principle and method are described in detail in the literature [17]. Fig. 2(a) depicts a cross section of the LFB acoustic lens and the specimen, illustrating the measurement principle. When the distance z between the LFB acoustic lens and the specimen is changed in the characterization region from -560 to $+60$ μm, a V(z) curve recorded as a transducer output exhibits an interference waveform, as shown in Fig. 3(a), in which the two components of #0 and #1 in Fig. 2(a) effectively contribute to the transducer output. Based on the analytical procedure of the V(z) curve analysis [17], the interference component of the $V_I(z)$ curve [Fig. 3(b)] is obtained by extracting the characteristic lens response $V_L(z)$, indicated by the dotted line, from the V(z) curve in Fig. 3(a). A fast Fourier transform (FFT) analysis then is performed on this waveform to obtain the spectral distribution $F(k)$ [Fig. 3(c)]. The interference interval Δz is subsequently determined from its peak wave number. The phase velocity of the LSAWs, V_{LSAW}, is obtained by substituting Δz into (1):

$$V_{LSAW} = \frac{V_W}{\sqrt{1 - \left(1 - \dfrac{V_W}{2f \cdot \Delta z}\right)^2}}, \qquad (1)$$

where V_W is the velocity of the longitudinal waves in water.

An ultrasonic beam formed on the specimen surface by the LFB ultrasonic device is depicted in Fig. 2(b), and LSAWs propagate in the x direction. The LSAW propagation distance W in the focused direction in the measurement region is given by $2|z| \tan \theta_{\mathrm{LSAW}}$, where z is the defocus distance in the V(z) curve and θ_{LSAW} is the critical angle for the LSAWs, defined as $\theta_{\mathrm{LSAW}} = \sin^{-1} V_w/V_{\mathrm{LSAW}}$. The maximum z used for analysis of LSAWs on C-7972 specimens is -275 μm, and the maximum W is then 280 μm. In contrast, the effective beam width D in the unfocused direction in the measurement region depends on the performance parameters of the ultrasonic device. The dimensions of the acoustic lens used for the measurements in this paper were as follows: the curvature radius of the cylindrical lens was 1 mm, the aperture half-angle was 60°, and the rod length was 12 mm. The transducer widths were 1.73 mm in the focused direction and 1.50 mm in the unfocused direction. This device operated in a frequency range from 100 to 300 MHz. D was approximately 900 μm. The resolution in the depth direction was estimated to be approximately 15 μm at 225 MHz because most of the LSAWs' energy was confined within a wavelength below the surface as they propagated.

IV. Experiments and Discussions

A. Inhomogeneity Evaluation

1. Angular Dependence: The angular dependences of the LSAW velocity were measured at a single point near the center of the specimens because TiO_2-SiO_2 glass has structural anisotropy due to its striae. The results are presented in Fig. 4. The LSAW propagation direction perpendicular to the striae plane [z direction in Fig. 1(c)] was taken as 0° for specimens A-2 and B-2, and in the x direction in Fig. 1(b) it was 0° for specimens A-1 and B-1. A significant LSAW velocity variation was observed in specimen A-2 in the neighborhood of 0°, and the maximum velocity difference obtained for the angular dependence was 1.16 m/s. A slight velocity variation of 0.44 m/s was observed in specimen B-2. The velocity variations obtained for specimens A-1 and B-1 were each less than 0.44 m/s. The angular dependences obtained for specimens A-2 and B-2 evidently responded to their structure of striae in the specimen configuration, as indicated in Fig. 1(c).

2. Two-Dimensional Distribution: The two-dimensional distributions of LSAW velocities then were measured for the surfaces of the four specimens; the results are provided in Fig. 5(a). The LSAW velocities were measured for the z-axis wave propagation in 0.05-mm steps in the z direction and in 0.5-mm steps in the y direction for an area of 2 mm × 2 mm for specimens A-2 and B-2, for the x-axis wave propagation in 1-mm steps in the x direction and in 2-mm steps in the y direction for an area of 34 mm × 48 mm for specimen A-1, and in 1-mm steps in both the x and y directions for an area of 14 mm × 84 mm for specimen B-1. The averaged LSAW velocities were 3307.90 m/s, 3308.28 m/s, 3307.34 m/s, and 3308.09 m/s for specimens A-1, A-2, B-1, and B-2, with maximum velocity differences of 12.83 m/s, 3.74 m/s, 2.66 m/s, and 0.94 m/s. The LSAW velocity distributions were measured for two LSAW propagation directions parallel and perpendicular to the measurement lines indicated by the dotted line in Fig. 5(a); the results are indicated by the solid and dotted lines in Fig. 5(b). Nearly the same velocity distributions were observed in both directions for specimens A-1 and B-1. Periodic velocity distributions were observed for the LSAW propagation direction perpendicular to the striae plane for specimens A-2 and B-2; the velocity variations were larger than those obtained for the LSAW propagation direction parallel to the striae plane. Larger variations in the velocity distributions were observed for the specimens cut from the premium-grade ingot than for those from the mirror-grade ingot.

A velocity difference of 12.83 m/s was obtained for specimen A-1 in the two-dimensional LSAW velocity distribution. The measured values of the LSAW velocity varied considerably, depending on which section in the striae layers with periodic changes in the TiO_2 concentration happened to be at the surface of the specimen, due to the fact that the striae plane was not completely flat but curved, the periodicity of the LSAW velocity variations was sufficiently larger than the LSAW propagation distance of the maximum W (280 μm), and the wavelength of the LSAWs (15 μm at 225 MHz) was much shorter than the periodicity of the striae (about 0.17 mm). Similar but much smaller LSAW velocity variations also were observed for specimen B-1.

A velocity distribution was clearly detected by FFT analysis of specimen A-2, with an average periodicity of 0.168 mm. Similar periodic velocity distributions were observed for specimen B-2 with the same periodicity of 0.168 mm in a region from $z = -0.5$ mm to 1.0 mm, though the velocity variations were somewhat small. Fig. 6 illustrates the relationship between the measurement region ($W \times D$) with the LFB acoustic lens and the periodic striae at $z = -275$ μm for the perpendicular specimens whose surfaces were prepared perpendicular to the striae plane, as indicated in Fig. 1(c), such as specimens A-2 and B-2. The results illustrated with the solid lines in Figs. 5(B-b) and 5(D-b) correspond to the measurement in Fig. 6(a), and those depicted with dotted lines in Figs. 5(B-b) and 5(D-b) correspond to the measurement in Fig. 6(b). When LSAWs propagated perpendicular to the striae plane, as shown in Fig. 6(a), the maximum W in the measurement region (280 μm at $z = -275$ μm) was slightly larger than the periodicity of the striae (0.17 mm). Therefore, subtle periodic changes in acoustic properties on the perpendicular specimen surface were detected as LSAW velocity variations when the measurement region was moved in a direction perpendicular to the striae plane, as plotted by the solid lines in Figs. 5(B-b) and 5(D-b). In this case, the surface characteristics over the striae layers of approximately

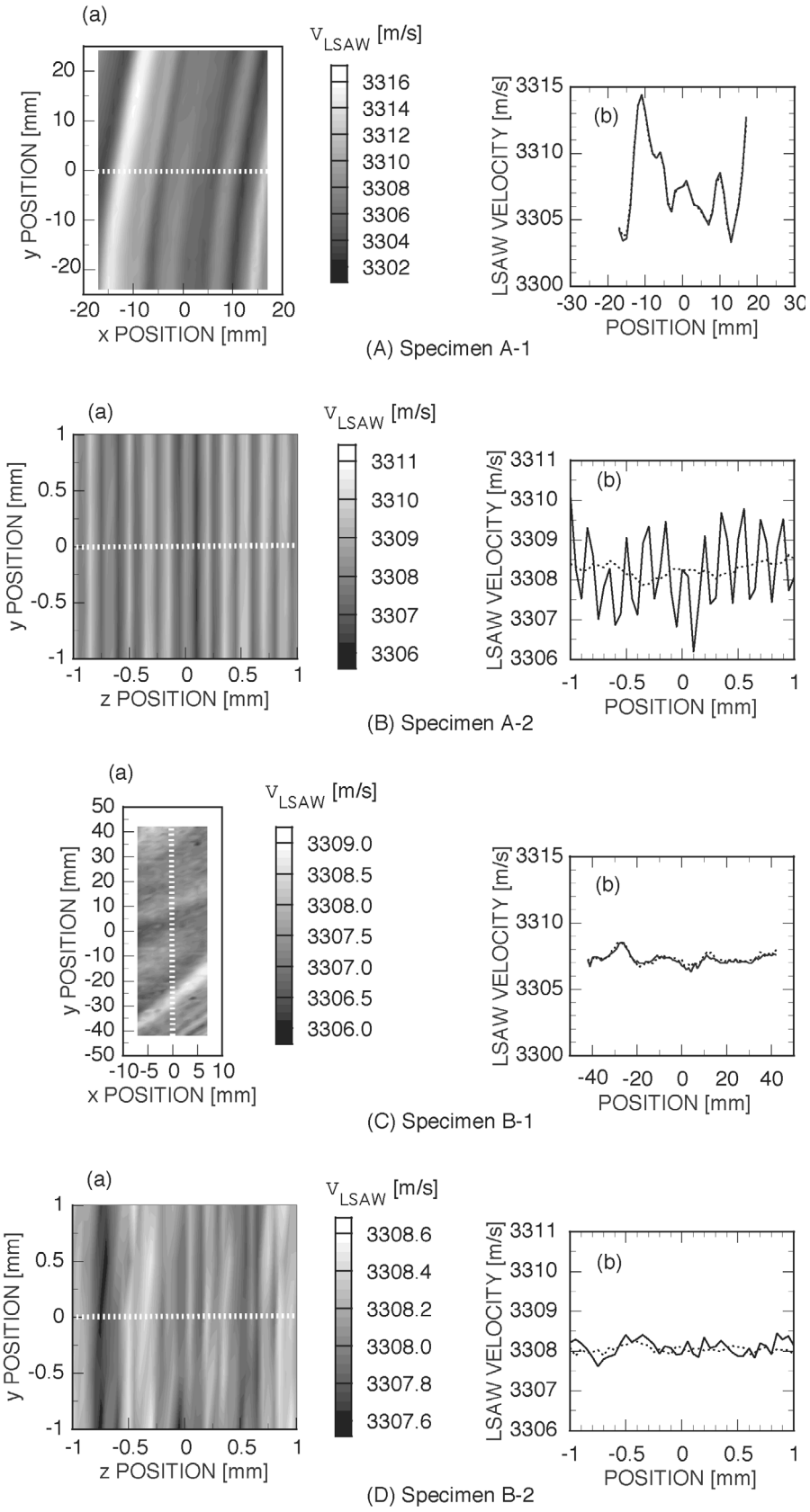

Fig. 5. LSAW velocity profiles of specimens A-1, A-2, B-1, and B-2 of C-7972 at 225 MHz. (a) Two-dimensional distributions. (b) Distributions along $y = 0$ (dotted line) for (A), (B), and (D), and along $x = 0$ (dotted line) for (C) in (a). LSAWs propagated in the z-axis direction in (B-a) and (D-a).

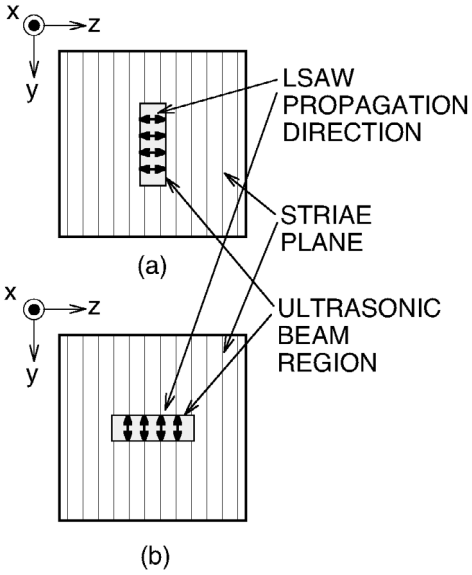

Fig. 6. Relationships between the measurement region with the LFB acoustic lens and the periodic striae at $z = -275$ μm for the perpendicular specimens in Fig. 1(c). (a) LSAWs propagated perpendicular to the striae plane. (b) LSAWs propagated parallel to the striae plane.

1.7 periodicities were averaged, resulting in smaller velocity variations for specimen A-2 (B-2) than for specimen A-1 (B-1). In contrast, the LSAW velocities were measured as the averaged values of their characteristics when the LSAWs propagated parallel to the striae plane, as illustrated in Fig. 6(b), because the ultrasonic beam width in the unfocused direction in the measurement region was approximately five times greater than the periodicity of the striae. Hence, the measured results plotted with dotted lines signify much smaller velocity variations than those plotted with solid lines, as illustrated in Figs. 5(B-b) and 5(D-b).

The above experimental results led us to conclude that parallel specimen substrates are useful with LSAW velocity measurements for evaluating intrinsic property changes of the material itself. Perpendicular specimen substrates are useful with LSAW velocities in a propagation direction perpendicular to the striae plane for measuring the periodicity of striae, and with LSAW velocities in a propagation direction parallel to the striae plane for obtaining the averaged properties of specimens.

The sensitivities of the LSAW velocity to the TiO_2 concentration and CTE are reportedly -0.058 wt%/(m/s) and 4.40 (ppb/K)/(m/s) [27]. The measurement results in Fig. 5 indicate that the maximum velocity variation for the premium-grade ingot was a TiO_2 concentration variation of 0.75 wt% and a CTE variation of 56.45 ppb/K and that the velocity variation for the mirror-grade ingot was a TiO_2 concentration variation of 0.15 wt% and a CTE variation of 11.70 ppb/K. The velocity variation detected for this ingot was almost six times larger because the specification of the CTE distribution in the premium-grade ingot was within 10 ppb/K. Thus, the striae formed due to changes in the chemical compositions in the premium-grade ingot used in this investigation are much more serious than those in the mirror-grade ingot because the premium-grade ingot was supposedly of higher quality. This is considered to be due to the fact that the manufacturer uses the longitudinal velocity measurements for quality control. The manufacturer evaluates the CTE of the glass ingots by measuring the velocities of longitudinal waves propagating in the thickness direction of the ingot (i.e., perpendicular to the striae plane), as indicated in Fig. 1(a), and uses the two-dimensional distribution of the averaged velocities [14]–[16]. This may explain why the Corning data differed from the LSAW velocity distributions on the specimen surfaces caused by the striae measured by our method.

B. Selection of a Standard Specimen

Homogeneous standard specimens would be ideal for calibrating the LFB-UMC system. However, TiO_2-SiO_2 glass has striae, which cause periodic velocity variations, as indicated by the experimental results. A method for selecting a standard specimen was discussed to address this problem.

We assumed that our measurements of the velocities of the bulk waves for parallel specimens yielded the averaged characteristics of several tens of striae layers for the bulk-wave propagation in the thickness direction of the substrate. However, significant distributions of the LSAW velocities were detected, particularly for specimen A-1 (12.83 m/s), resulting in an absolute uncertainty in the measured values. Similarly, the measured values for specimen B-1, which exhibited a smaller velocity variation on the specimen surface than specimen A-1, contained an uncertainty of 2.66 m/s. Therefore, these specimens are not appropriate as standard specimens.

The averaged characteristics of more than 10 layers of the striae are thought to be measured when the velocities of bulk waves are measured for perpendicular specimens because the diameter of bulk-wave transducers (typically 2.5 mm at 200 MHz) is much larger than the periodicity of striae (0.17 mm). The averaged characteristics of LSAW velocities also can be obtained for LSAW propagation parallel to the striae plane on perpendicular specimens, as illustrated in Figs. 5(B-b) and 5(D-b), and they do not depend strictly upon the measurement positions. Therefore, perpendicular specimens are most useful for accurate system calibration. In addition, specimen B-2 is considered to be more suitable as a standard specimen than specimen A-2 because the former exhibited a smaller velocity variation.

C. Acoustic Properties of the Standard Specimen

1. Standard of LSAW Velocity: It is necessary to measure two velocities of proper longitudinal and shear waves to calculate a standard velocity of Rayleigh-type LSAWs on the surface of a standard specimen. The LSAW's particle motion consists of two components: a longitudinal com-

ponent and a shear component with a particle displacement perpendicular to the specimen surface. The LSAWs for the standard specimens selected above propagate in a direction (y axis) parallel to the striae plane on the specimen surface that was prepared perpendicular to the striae plane, as illustrated in Fig. 1(c). These two velocities of longitudinal and shear waves can be measured with averaged values for both specimens A-2 and B-2.

To use specimens A-2 and B-2 as standard specimens, we measured the two bulk-wave velocities in a frequency range of 50 to 270 MHz using two plane-wave ultrasonic devices for longitudinal- and shear-wave modes instead of the LFB-focused ultrasonic device in the measurement system. The measurement method is described in detail in the literature [34]. The diffraction effects in the velocity measurements were corrected [34] with numerical calculations using the exact integral expression of Williams [35].

Figs. 7(a) and (b) depict the results measured at 23°C for each specimen. Nearly the same values were obtained in specimen B-2 for both the longitudinal and shear velocities in the measurement frequency range; slight velocity variations, apparent frequency dependences, were observed for specimen A-2 due to its layered structure with a greater degree of striae and the fact that the striae plane may not have been completely perpendicular to the substrate surface. Fig. 7(c) presents the results measured at 20, 23, and 26°C for specimen B-2. The approximated straight lines given by the least-squares method revealed that the temperature coefficients of the longitudinal and shear velocities were +0.75 (m/s)/°C and +0.30 (m/s)/°C. The densities were obtained using the Archimedes method [36] as 2197.76 kg/m^3 for specimen A-2 and 2197.74 kg/m^3 for specimen B-2. Their temperature coefficients were negligible due to the ultra-low expansion glass. The LSAW velocities were calculated from these results according to the method in the literature [37], [38], and the results at 23°C are provided in Fig. 8. The calculated results of the LSAW velocities reflect the characteristics of the bulk acoustic waves; very little velocity dispersion was obtained for specimen B-2, with an average standard LSAW velocity of 3308.18 m/s with a maximum difference of 0.08 m/s in the frequency range. An apparent velocity dispersion was obtained for specimen A-2 with a maximum velocity change of 0.32 m/s. The temperature coefficient of the LSAW velocities for specimen B-2 was determined to be +0.39 (m/s)/°C, around room temperature, through numerical calculations using the measured temperature dependences of the longitudinal and shear velocities in Fig. 7(c).

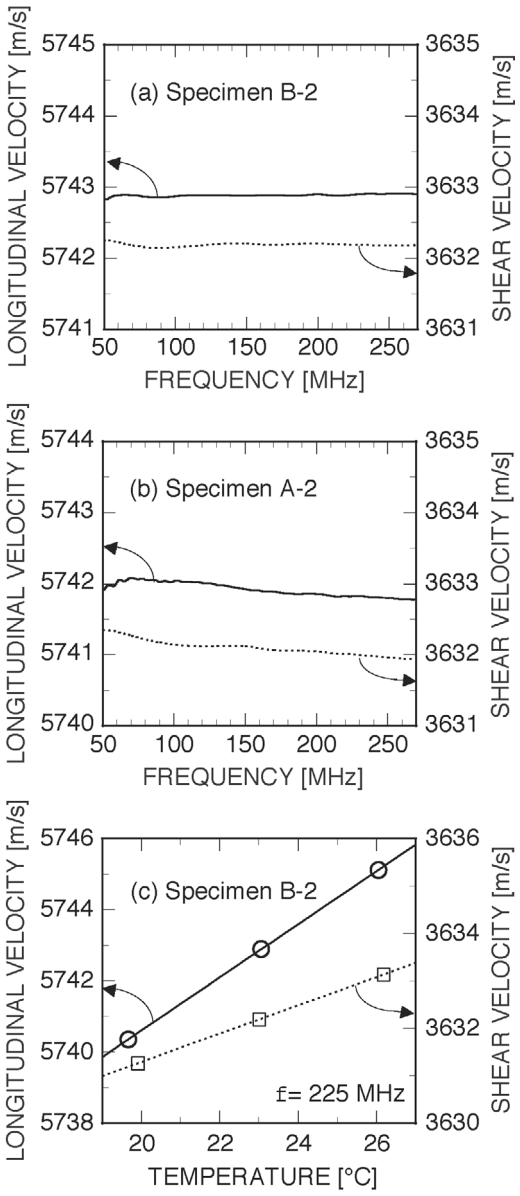

Fig. 7. Bulk acoustic wave (BAW) velocities measured for standard specimens of C-7972. Dispersion of BAW velocities for (a) specimen B-2 and (b) specimen A-2 at 23°C. (c) Temperature dependences of BAW velocities for specimen B-2 at 225 MHz. Solid lines and circles, longitudinal wave velocities; dotted line and squares, shear wave velocities.

2. Uncertainty of the Standard LSAW Velocity: If substrates with LSAW velocity distributions on their surfaces are used as standard specimens for calibrating the LFB-UMC system, the LSAW velocity used as a reference could vary more or less with the placement position or angle of the standard specimen for calibration. Fig. 9(a) depicts the results of a two-dimensional velocity measurement of LSAWs propagating parallel to the striae plane for specimen B-2, conducted at 23°C in 0.1 mm steps for an area of 2×2 mm in the y and z directions. The average LSAW velocity was 3308.20 m/s, with a maximum difference of 0.47 m/s. The maximum LSAW velocity difference obtained for an area of 1 mm × 1 mm was 0.44 m/s, and that for an area of 0.4 mm × 0.4 mm was 0.27 m/s. Our experimental experience suggests that it is simple to adjust the center of the measurement region for calibration within an area of 0.4 mm × 0.4 mm; the effect caused by deviation from the proper placement position of standard specimen B-2 was estimated to be within 0.27 m/s.

Additional measurements were conducted in 0.1 mm steps for an area of 0.4 mm × 0.4 mm in the y and z

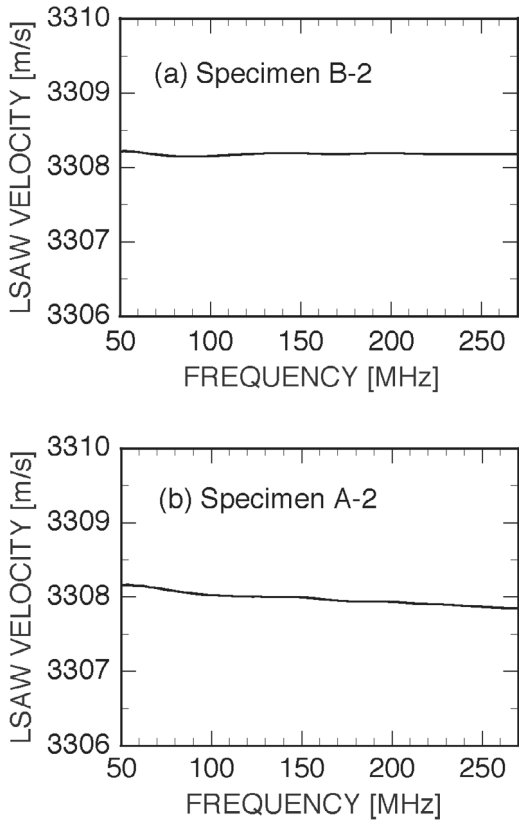

Fig. 8. Dispersion of LSAW velocities numerically calculated using the measured data of BAW velocities in Fig. 7 for C-7972 standard specimens at 23°C. (a) Specimen B-2. (b) Specimen A-2.

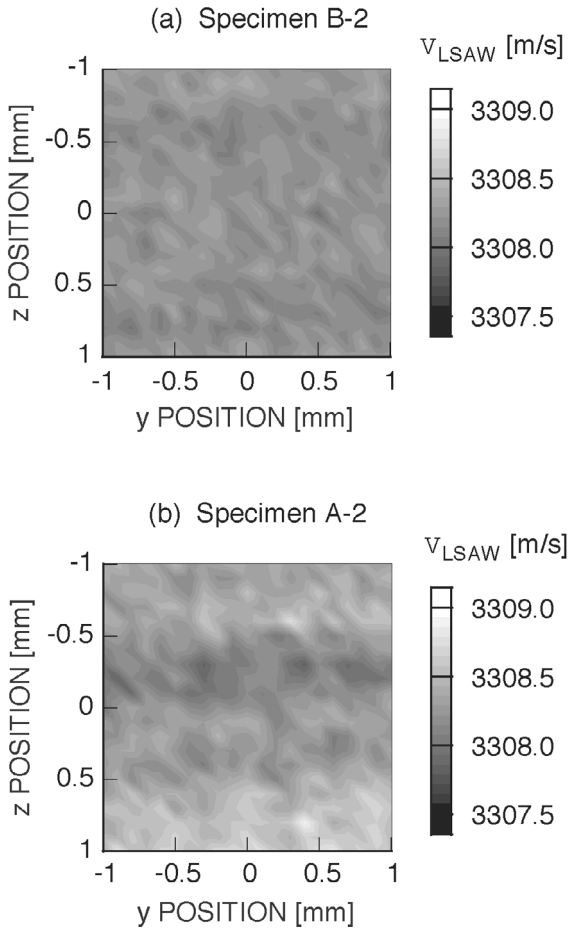

Fig. 9. Two-dimensional velocity distributions for LSAW propagation direction (y-axis) parallel to the striae plane on the perpendicular specimens at 225 MHz. (a) Specimen B-2. (b) Specimen A-2.

directions with the specimen rotated by 2, 5, and 10°. The averaged LSAW velocities obtained were nearly the same, at 3308.13 m/s, 3308.14 m/s, and 3308.15 m/s, with maximum velocity differences of 0.35 m/s, 0.25 m/s, and 0.24 m/s. These results demonstrate that the placement angle has almost no effect on the measured velocity values if the angle is within ±10°. Therefore, an absolute LSAW velocity of 3308.18 m/s within ±0.21 m/s can be obtained from the experimental results for a standard specimen placed within ±0.2 mm and ±10° around its center. The measurement reproducibility obtained from 200 successive LSAW velocity measurements was ±0.14 m/s (±0.0041%) for $\pm 2\sigma$ (σ: standard deviation), which indicates that the uncertainty of the standard LSAW velocity is nearly equal to the reproducibility for specimen B-2.

Similarly, Fig. 9(b) presents the results of a two-dimensional measurement of LSAW velocities for an area of 2 mm × 2 mm on the surface of specimen A-2. The averaged LSAW velocity was 3308.33 m/s, with a maximum difference of 1.04 m/s. The velocity distribution of specimen A-2 was greater than that of specimen B-2; however, it was less than one-third of that obtained for the LSAW propagation direction perpendicular to the striae plane [Fig. 5(B-a)], indicating that the characteristics of the specimen were averaged. Although homogeneous specimens would be ideal standard specimens, a proper and acceptable standard can be obtained for specimens with periodic inhomogeneity due to their striae by using a perpendicular specimen in which the LSAWs travel parallel to the striae plane.

The LSAW velocities obtained in the measurements of Section IV were calibrated using the standard specimen B-2 on which LSAWs propagated parallel to the striae plane. The standard LSAW velocity was 3308.18 ± 0.35 m/s at 23°C with its temperature coefficient of 0.39 (m/s)/°C.

V. Summary

This paper investigated experimental procedures and standard specimens suitable for characterizing and evaluating TiO_2-SiO_2 ultra-low expansion glasses with periodic striae using the LFB-UMC system. The LSAW velocities were measured at 225 MHz for specimens prepared from two different grades of commercial glass ingots with substrate surfaces prepared either parallel or perpendicular to the striae plane. Velocity variations associated with the degree of striae were accurately detected for the parallel specimens. Different velocity distributions were observed for the perpendicular specimens, depending on the propagation direction. A velocity distribution with a striae pe-

riodicity of about 0.17 mm was detected for an LSAW propagation direction perpendicular to the striae plane, and a very small velocity distribution was observed for an LSAW propagation direction parallel to the striae plane. These results were reviewed from the perspective of the measurement region of the LFB ultrasonic device used, and a method for selecting appropriate standard specimens was investigated. We clarified that standard specimens with substrate surface preparation perpendicular to the striae plane and an LSAW propagation parallel to the striae plane on their surfaces are most appropriate to provide an accurate standard of the LSAW velocity. The averaged characteristics on the substrate surfaces were measured and uncertainty of the standard due to striae was reduced in these specimens, resulting in a reliable standard with almost no effect of the striae. We also investigated the effects of deviations from the placement position and angle of the standard specimen. The standard of LSAW velocity for calibrating the LFB-UMC system was obtained through numerical calculations using the measured data of longitudinal- and shear-wave velocities and density for the standard specimen. A standard value of an LSAW velocity of 3308.18 ± 0.35 m/s at 23°C was provided for specimen B-2, which had a small velocity variation on its surface. This included a measurement error of ± 0.14 m/s for $\pm 2\sigma$ at a single position and can be used to evaluate TiO_2-SiO_2 ultra-low expansion glass. The temperature coefficient was +0.39 (m/s)/°C. The LSAW velocity of 3308.18 m/s at 23°C can be used for TiO_2-SiO_2 ultra-low expansion glass with a TiO_2 concentration of 7.09 wt%, based on the relationship between them determined elsewhere [39]. The uncertainty of ± 0.35 m/s in the standard value is significantly less than the maximum velocity variation of 2.66 m/s due to the striae observed in the specimens from the glass-ingot B.

The mirror-grade ingot used in the measurements in this paper exhibited smaller LSAW velocity distributions than the premium-grade ingot that we used, which is contrary to the technical information provided by the manufacturer. This is most likely due to the fact that the manufacture's quality control of CTE is based on the distribution of the averaged longitudinal bulk-wave characteristics along the thickness direction of the specimen substrate; the characteristics on the specimen surfaces are obtained for LSAWs in our method. This will be investigated further in the future.

References

[1] H. Wang, N. Yamada, and M. Okaji, "Thermal expansion of some silica glasses in the range from −50 to 250°C by push-rod dilatometry," *AIST Bull. Metrology*, vol. 1, pp. 77–85, Jan. 2002.

[2] P. C. Schultz and H. T. Smyth, "Ultra-low-expansion glasses and their structure in the SiO_2-TiO_2 system," in *Amorphous Materials*. R. W. Douglas and B. Ellis, Eds. New York: Wiley-Intersci., 1970, pp. 453–461.

[3] R. B. Greegor, F. W. Lytle, D. R. Sandstrom, J. Wong, and P. Schultz, "Investigation of TiO_2-SiO_2 glasses by X-ray absorption spectroscopy," *J. Non-Cryst. Solids*, vol. 55, pp. 27–43, 1980.

[4] R. Haug, W. Heimerl, R. Hentschel, H. Höness, A. Jacobsen, K. Knapp, E.-D. Knohl, T. Marx, H. Morian, R. Müller, W. Pannhorst, N. Reisert, B. Speit, and A. Thomas, "Zerodur®—A low thermal expansion glass ceramic for optical precision applications," in *Low Thermal Expansion Glass Ceramics*. H. Bach, Ed. Berlin: Springer, 1995, pp. 107–214.

[5] D. Gerlich and M. Wolf, "Thermoelastic properties of Zerodur® glass-ceramic," *J. Non-Cryst. Solids*, vol. 27, pp. 209–214, 1978.

[6] N. P. Bansal and R. H. Doremus, "Elastic properties," in *Handbook of Glass Properties*. Orlando, FL: Academic, 1986, pp. 306–336.

[7] R. Brückner, "Properties and structure of vitreous silica. I," *J. Non-Cryst. Solids*, vol. 5, pp. 123–175, 1970.

[8] W. P. Mason and H. J. McSkimin, "Attenuation and scattering of high frequency sound waves in metals and glasses," *J. Acoust. Soc. Amer.*, vol. 19, pp. 464–473, May 1947.

[9] S. Spinner, "Elastic moduli of glasses at elevated temperatures by a dynamic method," *J. Amer. Ceram. Soc.*, vol. 39, pp. 113–118, Mar. 1956.

[10] S. Spinner, "Temperature dependence of elastic constants of vitreous silica," *J. Amer. Ceram. Soc.*, vol. 45, pp. 394–397, Aug. 1962.

[11] J. E. Shelby, Jr., and D. E. Day, "Mechanical relaxations in mixed-alkali silicate glasses: I. Results," *J. Amer. Ceram. Soc.*, vol. 52, pp. 169–174, Apr. 1969.

[12] J. E. Shelby, Jr., and D. E. Day, "Mechanical relaxations in mixed-alkali silicate glasses: II. Discussion," *J. Amer. Ceram. Soc.*, vol. 53, pp. 182–187, Apr. 1970.

[13] K. Nassau, J. W. Shiever, and J. T. Krause, "Preparation and properties of fused silica containing alumina," *J. Amer. Ceram. Soc.*, vol. 58, p. 461, Sep.–Oct. 1975.

[14] H. E. Hagy, "High precision photoelastic and ultrasonic techniques for determining absolute and differential thermal expansion of titania-silica glasses," *Appl. Opt.*, vol. 12, pp. 1440–1446, July 1973.

[15] H. E. Hagy and W. D. Shirkey, "Determining absolute thermal expansion of titania-silica glasses: A refined ultrasonic method," *Appl. Opt.*, vol. 14, pp. 2099–2103, Sep. 1975.

[16] M. J. Edwards, E. H. Bullock, and D. E. Morton, "Improved precision of absolute thermal expansion measurements for ULE™ glass," *Proc. SPIE, Adv. Mater. Opti. Precision Struct.*, vol. 2857, pp. 58–63, 1996.

[17] J. Kushibiki and N. Chubachi, "Material characterization by line-focus-beam acoustic microscope," *IEEE Trans. Sonics Ultrason.*, vol. SU-32, pp. 189–212, Mar. 1985.

[18] J. Kushibiki, Y. Ono, Y. Ohashi, and M. Arakawa, "Development of the line-focus-beam ultrasonic material characterization system," *IEEE Trans. Ultrason., Ferroelect., Freq. Contr.*, vol. 49, pp. 99–113, Jan. 2002.

[19] J. Kushibiki, H. Asano, T. Ueda, and N. Chubachi, "Application of line-focus-beam acoustic microscope to inhomogeneity detection on SAW device materials," in *Proc. IEEE Ultrason. Symp.*, 1986, pp. 749–753.

[20] M. Kadota, T. Kitamura, and T. Kasanami, "Evaluation of glass substrates for SAW filters by acoustic microscopy technique," *Trans. IEE Jpn.*, vol. 111-C, pp. 412–418, Sep. 1991.

[21] C. K. Jen, C. Neron, A. Shang, K. Abe, L. Bonnell, and J. Kushibiki, "Acoustic characterization of silica glasses," *J. Amer. Ceram. Soc.*, vol. 76, pp. 712–716, Mar. 1993.

[22] Y. Ono, J. Kushibiki, and N. Chubachi, "Characterization of optical fiber preforms by line-focus-beam acoustic microscopy," in *Proc. IEEE Ultrason. Symp.*, 1993, pp. 1243–1246.

[23] J. Kushibiki, T. C. Wei, Y. Ohashi, and A. Tada, "Ultrasonic microspectroscopy characterization of silica glass," *J. Appl. Phys.*, vol. 87, pp. 3113–3121, Mar. 2000.

[24] J. Kushibiki and A. Tada, "Ultrasonic micro-spectroscopy characterization of silica glasses," Tech. Rep. IEICE, Tokyo, Japan, vol. US99-67, pp. 1–8, Dec. 1999.

[25] A. Tada and J. Kushibiki, "Evaluation of fused quartz glass fabrication process by ultrasonic micro-spectroscopy," Rep. Spring Mtg. Acoust. Soc. Japan, Tokyo, Japan, pp. 835–836, Mar. 2000.

[26] J. Kushibiki, M. Arakawa, Y. Ohashi, and R. Okabe, "Evaluation of glass materials by using the line-focus-beam ultrasonic-material-characterization system," *IEEE Trans. Ultrason., Ferroelect., Freq. Contr.*, vol. 52, pp. 1152–1160, July 2005.

[27] J. Kushibiki, M. Arakawa, Y. Ohashi, K. Suzuki, and T. Maruyama, "A promising evaluation method of ultra-low-

expansion glasses for the extreme ultra-violet lithography system by the line-focus-beam ultrasonic material characterization system," *Jpn. J. Appl. Phys.*, vol. 43, pp. L1455–L1457, Nov. 2004.
[28] J. Kushibiki, M. Arakawa, Y. Ohashi, K. Suzuki, and T. Maruyama, "A super-precise CTE evaluation method for ultra-low-expansion glasses using the LFB ultrasonic material characterization system," *Jpn. J. Appl. Phys.*, vol. 44, pp. 4374–4380, June 2005.
[29] Y. Ono and J. Kushibiki, "Experimental study of construction mechanism of V(z) curves obtained by line-focus-beam acoustic microscopy," *IEEE Trans. Ultrason., Ferroelect., Freq. Contr.*, vol. 47, pp. 1042–1050, July 2000.
[30] J. Kushibiki and M. Arakawa, "A method for calibrating the line-focus-beam acoustic microscopy system," *IEEE Trans. Ultrason., Ferroelect., Freq. Contr.*, vol. 45, pp. 421–430, Mar. 1998.
[31] J. Kushibiki, M. Arakawa, and R. Okabe, "High-accuracy standard specimens for the line-focus-beam ultrasonic material characterization system," *IEEE Trans. Ultrason., Ferroelect., Freq. Contr.*, vol. 49, pp. 827–835, June 2002.
[32] Y. Ohashi and J. Kushibiki, "Development of an improved calibration method for the LFB ultrasonic material characterization system," *IEEE Trans. Ultrason., Ferroelect., Freq. Contr.*, vol. 51, pp. 686–694, June 2004.
[33] K. E. Hrdina, B. Z. Hanson, P. M. Fenn, and R. Sabia, "Characterization and characteristics of a ULE® glass tailored for the EUVL needs," *Proc. SPIE, Emerging Lithographic Technol. VI*, vol. 4688, pp. 454–461, 2002.
[34] J. Kushibiki and M. Arakawa, "Diffraction effects on bulk-wave ultrasonic velocity and attenuation measurements," *J. Acoust. Soc. Amer.*, vol. 108, pp. 564–573, Aug. 2000.
[35] A. O. Williams, Jr., "The piston source at high frequencies," *J. Acoust. Soc. Amer.*, vol. 23, pp. 1–6, Jan. 1951.
[36] H. A. Bowman, R. M. Schoonover, and M. W. Jones, "Procedure for high precision density determinations by hydrostatic weighing," *J. Res. Nat. Bur. Stand.*, vol. 71C, pp. 179–198, July–Aug. 1967.
[37] I. A. Viktorov, *Rayleigh and Lamb Waves: Physical Theory and Applications*. New York: Plenum, 1967, pp. 46–57.
[38] J. J. Campbell and W. R. Jones, "Propagation of surface waves at the boundary between a piezoelectric crystal and a fluid medium," *IEEE Trans. Sonics Ultrason.*, vol. SU-17, pp. 71–76, Apr. 1970.
[39] M. Arakawa, J. Kushibiki, Y. Ohashi, and K. Suzuki, "Accurate calibration line for super-precise coefficient of thermal expansion evaluation technology of TiO_2-doped SiO_2 ultra-low expansion glass using the line-focus-beam ultrasonic material characterization system," *Jpn. J. Appl. Phys.*, vol. 45, pp. 4511–4515, May 2006.

Jun-ichi Kushibiki (M'83) was born in Hirosaki, Japan, on November 23, 1947. He received the B.S., M.S., and Ph.D. degrees in electrical engineering from Tohoku University, Sendai, Japan, in 1971, 1973, and 1976, respectively.

In 1976 he became a research associate at the Research Institute of Electrical Communication, Tohoku University. In 1979, he joined the Department of Electrical Engineering, Faculty of Engineering, Tohoku University, where he was an associate professor from 1988 to 1993 and became a professor in 1994. He has been studying ultrasonic metrology, especially acoustic microscopy and its applications, and established a method of material characterization by line-focus-beam acoustic microscopy. He also has been interested in biological tissue characterization in the higher frequency range, applying both bulk and acoustic microscopy techniques.

Dr. Kushibiki is a Fellow of the Acoustical Society of America; a Member of the Institute of Electronics, Information and Communication Engineers of Japan, of the Institute of Electrical Engineers of Japan, of the Acoustical Society of Japan, of the Japan Society of Ultrasonics in Medicine, and of the Japan Society of Applied Physics.

Mototaka Arakawa (M'00) was born in Sendai, Japan, on January 19, 1971. He received the B.S., M.S., and Ph.D. degrees in electrical engineering from Tohoku University, Sendai, Japan, in 1993, 1995, and 2000, respectively.

In 2000, he became a Center of Excellence Research Fellow at the Research Institute of Electrical Communication, Tohoku University. In 2001, he became research associate at the Department of Electrical Engineering, Faculty of Engineering, Tohoku University. His research interests include development of the measurement methods of elastic constants of solid materials and of the calibration method of the line-focus-beam acoustic microscopy system.

Dr. Arakawa is a member of the Acoustical Society of Japan, of the Institute of Electronics, Information and Communication Engineers of Japan, and of the Japan Society of Applied Physics.

Yuji Ohashi was born in Toyama Prefecture, Japan, on August 27, 1973. He received the B.S., M.S., and Ph.D. degrees in electrical engineering from Tohoku University, Sendai, Japan, in 1996, 1999, and 2003, respectively.

In 2003 he became a Center of Excellence Fellow (postdoctoral) at the Department of Electronics, Graduate School of Engineering, Tohoku University. His research interests include development of line-focus-beam acoustic microscopy system and its applications to materials characterization.

Dr. Ohashi is a member of the Acoustical Society of Japan and of the Japan Society of Applied Physics.